

# Behaviour of the aluminium oxide layer during heat treatment and the resulting effects on brazeability

M. Lohrey · U. Fuessel · M. Tuerpe

Received: 16 December 2013 / Accepted: 6 October 2014 / Published online: 24 October 2014  
© International Institute of Welding 2014

**Abstract** During the last years, the trend to develop lighter products becomes more and more important in the automotive industry. In case of reduction of the material thicknesses, the joining technologies become more important as well and lead to a request for higher process reliability. This is also happening in the field of aluminium brazing with shielding gas. In the manufacturing of aluminium heat exchangers as well as other components comprised of product line-up by BEHR, the automotive industry systems partner, the NOCOLOK flux brazing technology (non-corrosive lok), i.e., the gas-shielded brazing of aluminium materials, is consistently state of the art. To date, the joining of aluminium materials as necessary in the manufacturing processes of aluminium products has always posed a challenge, due to aluminium's high affinity for oxygen. The implementation of fluxing agents during the aluminium brazing and soldering processes eliminates the formation of oxide layers on the component surface, and surface reoxidation is prevented via a shielding-gas atmosphere. The said shielding-gas atmosphere is provided using nitrogen. In practice, the build-up of humidity and oxygen content in the shielding-gas atmosphere cannot be totally prevented. The increasingly complex brazing products require continuous brazing-process improvements. In order to fulfil this requirement, sensitivity analyses relating to oxide layer build-up have been set up. In particular, the impact of oxygen and humidity in the brazing protective atmosphere as well as the influence of humidity on the aluminium surface are hereby closely examined. The retaining water model describes the interaction

of the aluminium surface and the process of water treatment and leads as a important key factor for a higher understanding of the behaviour of the aluminium oxide during heat treatment and the resulting effect on brazeability.

**Keywords** Heat treatment · Aluminium · Oxides · Brazeability · Welded joints

## 1 Introduction

The influence of water on the surfaces of aluminium, an aluminium alloys, is an interesting and continually well-researched field of knowledge since the onset of industrial-scale processing and production of aluminium.

In her paper, J. Zähr [1] addresses *inter alia* the behaviour of natural aluminium surface layers under different storage conditions, whereby amongst other issues she investigates the effects of humidity and condensation during the storage process on subsequent brazeability. She concludes that the primary cause for diminished test series soldering quality is not the increased oxide and/or hydroxide layer but rather the water that is physically retained by the surface layer, which then evaporates when subjected to temperatures in excess of 100 °C.

Furthermore, it is pointed out that this evaporation process occurs simultaneously to the transformation from hydroxide into oxide. Zähr thereby concludes that it is not only the thickness of the oxide layer and/or of the hydroxide layer that are significant, but that it is rather the water that is physically retained by the surface layer that is decisive to brazing and surmises that the evaporation of the moisture that has been physically retained leads to localised increases in brazing atmosphere humidity in the immediate vicinity of the potential soldered joint. This, surmises Zähr, interferes with the brazing process. Follow-up activities based on this paper concentrate,

Doc. IIW-2510, recommended for publication by Commission XVII  
“Brazing, Soldering, and Diffusion Bonding

M. Lohrey (✉) · M. Tuerpe  
MAHLE Behr GmbH, Stuttgart, Germany  
e-mail: Markus.Lohrey@MAHLE.com

U. Fuessel  
Dresden University of Technology, Dresden, Germany

amongst other things, on the impact of humidity and condensation occurring under industrial gas-shielded brazing process conditions whereby the key aspect lies both within the analysis of the influence wielded by humidity and oxygen in temperatures ranging up to approximately 600 °C and the resulting brazeability of aluminium materials [2].

## 2 Aluminium oxide layers

The characteristics of aluminium oxide layer have a main effect on the behaviour of aluminium material. The aluminium oxide layer passivates the aluminium or the aluminium alloy and, as a consequence, shields the base material [3, 4]. The natural aluminium oxide layer is actually composed of two layers superimposed on the top of one another on the aluminium surface. Directly on the aluminium base material, there is a 1- to 2-nm-thick barrier layer, on the top of which there is a 5- to 10-nm-thick coat layer [5–7].

The oxide layer on aluminium materials is very thin but, in comparison to other oxide layers, it is very dense and resistant [8, 9]. When eliminated, the oxide layer will build itself back up again in a few millisecond's time due to the effect of the oxygen. In one day's time, it will reach a thickness of 2–3 nm [10]. If stored for longer periods in humid atmospheres or in the event of exposure to temperature increases, this layer will keep building up. Aluminium oxide's melting temperature lies approximately around 2040 °C which is therefore far higher than the melting temperature of aluminium [9]. The thicker the aluminium oxide layer becomes, the slower it takes to grow due to the onset of an auto-inhibitory effect [10, 11].

## 3 Influence of humidity and oxygen contents in the atmosphere on oxide layer build-up

### 3.1 Test method description

The focus of the following experiment is the influence of different concentrations of humidity and oxygen on the oxidising effect occurring on aluminium when heated during a gas-shielded brazing process in nitrogen atmosphere is analysed and the resulting effects on brazeability are determined. To this purpose, whilst being heated in a laboratory brazing furnace (a so called glass furnace), aluminium samples are exposed to a specifically composed atmosphere (Table 1). The test gases are composed of different volumetric blends of the following base gases:

- Pure nitrogen
- Pure nitrogen with 50 ppm water
- Pure nitrogen with 100 ppm water
- Pure nitrogen with 3000 ppm oxygen

The said gases are appropriately blended for the experiment using a blender unit and then adjusted to the required test parameters by way of a measuring unit Figs. 1 and 2. Figure 3 provides a schematic view of the test installation layout. The samples are heated up to a temperature of 605 °C.

For the determination of the effects on the oxide layer, after cool-down to room temperature, the test samples are examined using FT-IR analysis techniques. In order to establish brazeability of the resulting sample surfaces, both the brazed test sample fillets and the soldering quality are evaluated (Figs. 1 and 2). Angle test specimens are thus applied (also compare Fig. 9).

The materials used for the brazing test samples comply with the aluminium alloys as generally implemented for current gas-shielded brazing processes. The base plate is composed of material item EN AW-3003 coated with brazing material item EN AW-4343. The V-shape is composed of uncoated material item EN-AW-3003.

### 3.2 Test results relating to oxide layer build-up

#### 3.2.1 Different oxygen concentrations in nitrogen, without humidity

Figure 4 displays the test sample results, determined without water contents in a nitrogen atmosphere. Oxygen content variations occurred between 12 and 200 ppm.

The values measured on a thermally untreated test sample are used as a reference for the individual test runs. Observation of Fig. 4 indicates that already with a 12 ppm oxygen content in the atmosphere; after the heating process, the oxide layer is 69 % thicker compared to the untreated test sample. Test performance with an oxygen content of 50 ppm once again results in a 19 % increase of the oxide layer. The integral value as measured at 50 ppm amounts to 3.2. A smaller oxide layer build-up occurs upon increasing of the oxygen content up to 100 ppm. Increasing the oxygen content up to 200 ppm does not lead to any further significant increase of the oxide layer thickness. Under the stated process conditions, the maximum oxide layer is thus already available with a 100 ppm oxygen content which will not increase any further, not even if the oxygen content is increased.

#### 3.2.2 Different oxygen concentrations in nitrogen with constant water contents of 50 ppm

Figure 5 displays the test sample results, determined in comparison to the previous experiments with respectively 50 ppm water contents in a nitrogen atmosphere. As in the previous experiments, oxygen content variations occur between 12 and 200 ppm. As already determined by the test series blends without water contents in the atmosphere (see above) here too, already with 12 ppm oxygen content and after the heating

**Table 1** Atmospheric test series blends

	12 ppm [O <sub>2</sub> ]	50 ppm [O <sub>2</sub> ]	100 ppm [O <sub>2</sub> ]	200 ppm [O <sub>2</sub> ]
0 ppm [H <sub>2</sub> O]	0 ppm H <sub>2</sub> O - 12 ppm O <sub>2</sub> - N <sub>2</sub> (remainder)	0 ppm H <sub>2</sub> O - 50 ppm O <sub>2</sub> - N <sub>2</sub> (remainder)	0 ppm H <sub>2</sub> O - 100 ppm O <sub>2</sub> - N <sub>2</sub> (remainder)	0 ppm H <sub>2</sub> O - 200 ppm O <sub>2</sub> - N <sub>2</sub> (remainder)
50 ppm [H <sub>2</sub> O]	50 ppm H <sub>2</sub> O - 12 ppm O <sub>2</sub> - N <sub>2</sub> (remainder)	50 ppm H <sub>2</sub> O - 50 ppm O <sub>2</sub> - N <sub>2</sub> (remainder)	50 ppm H <sub>2</sub> O - 100 ppm O <sub>2</sub> - N <sub>2</sub> (remainder)	50 ppm H <sub>2</sub> O - 200 ppm O <sub>2</sub> - N <sub>2</sub> (remainder)
100 ppm [H <sub>2</sub> O]	1100 ppm H <sub>2</sub> O - 12 ppm O <sub>2</sub> - N <sub>2</sub> (remainder)	100 ppm H <sub>2</sub> O - 50 ppm O <sub>2</sub> - N <sub>2</sub> (remainder)	100 ppm H <sub>2</sub> O - 100 ppm O <sub>2</sub> - N <sub>2</sub> (remainder)	100 ppm H <sub>2</sub> O - 200 ppm O <sub>2</sub> - N <sub>2</sub> (remainder)

process the oxide layer records its largest increase which now reaches 75 %. Performing the test with 50 ppm oxygen contents, the oxide layer is again 24 % higher compared to the 12 ppm test run with an integral value amounting to 3.1. Additional increases of the oxygen contents to 100 and 200 ppm do not result in any further increase in the oxide layer. Under the given process conditions, the maximum oxide layer is thus already available with a 50 ppm humidity and a 50 ppm oxygen content and it will not increase any further, not even if the oxygen content is increased.

### 3.2.3 Different oxygen contents in nitrogen with constant water contents of 100 ppm

Figure 6 displays the test sample results, determined in comparison to the previous experiment with water contents increased up to 100 ppm in a nitrogen atmosphere. As in the previous experiments, here too oxygen content variations again occur between 12 and 200 ppm. The test samples heated up to 12 ppm oxygen contents clearly display an augmented oxide layer with an integral value amounting to 3.5, corresponding to a layer build-up amounting to 118 % and thus, in comparison to the previous test series, resulting in the thickest oxide layer measured with the same oxygen contents. This value also gives maximum test results with 100 ppm water. Further oxygen content increases even result in a minimal retraction of the oxide layer to an average integral value of 3.3. What is particularly striking here is that the maximum oxide layer thickness is already reached with 12 ppm oxygen content. Under the given process conditions, the maximum

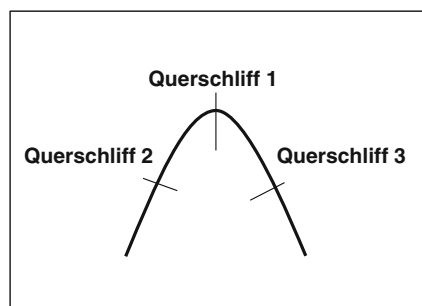
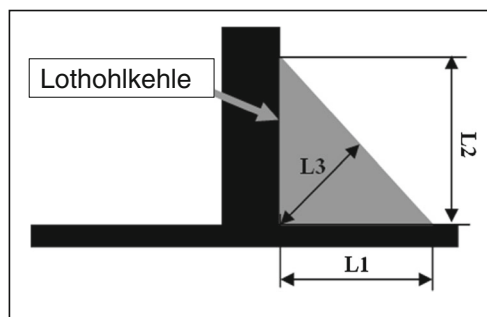
oxide layer is thus already available with a 100 ppm humidity and a 12 ppm oxygen content, and it will not increase any further, not even if the oxygen content is increased.

### 3.3 Consolidation of test results on oxide layer build-up

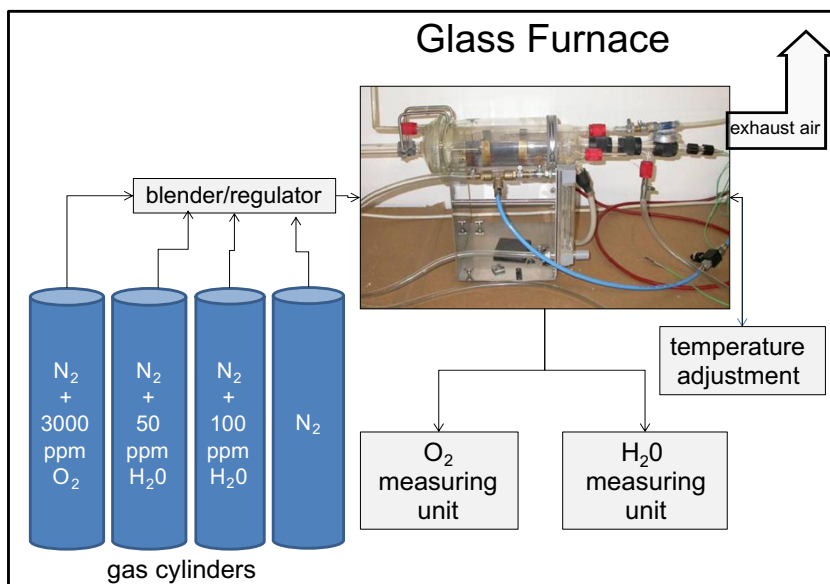
The aluminium oxide layer constitutes in itself a natural barrier to further oxide layer build-up and is capable of further reducing the diffusion process as its thickness is increased. The maximum oxide layer thickness is thus dependant on the temperature [12, 13]. In the tests performed, a maximum oxide layer thickness is reached at approximately the same level for all the test runs resulting in an integral value of 3.5. Figure 7 highlights this range with two dashed lines. This goes to show that at the preset process temperatures and process times, the maximum oxide layers occur on the test sample surfaces dependant on the atmospheric gas blends, with different oxygen and humidity concentrations.

The results also show that the maximum oxide layer thickness is reached with increased humidity contents in the atmosphere, at continually decreased oxygen values (Fig. 7). With increased humidity contents in the atmosphere, the oxygen needed in the same atmosphere to reach the maximum oxide layer values thus decreases. Whilst in an atmosphere without humidity an oxygen content of 100 ppm is required to reach the maximum oxide layer thickness, the required quantity drops to 12 ppm in an atmosphere having 100 ppm humidity content.

Based on the test series run, it is possible to reach the following conclusions:

**Fig. 1** Position of the test joint (left)**Fig. 2** Evaluation of the fillets (right)

**Fig. 3** Glass furnace gas blend experiments layout



1. Humidity contents in the atmosphere do not increase the maximum possible build-up of the oxide layer thickness (under otherwise similar conditions).
2. Humidity contents in the atmosphere reduce the oxygen contents required to reach the maximum possible oxide layer thickness (under otherwise similar conditions).

Figure 8 shows the correlation between humidity and oxygen contents in the atmosphere in relation to the maximum build-up of the oxide layer thickness. This figure clearly illustrates that in the course of a gas-shielded brazing process there is a build-up in the oxide layer whereby the maximum build-up of the oxide layer thickness is primarily dependant on the temperature. The diffusion processes and the diffusion speed as respectively required for build-up of the aluminium oxide are primarily dependant on the temperature and on the partial oxygen pressure. The test results show that in the

course of gas-shielded brazing processes, the maximum oxide layer thickness is reached only in the presence of sufficient oxygen contents performing as reactant partners. In the event that the necessary oxygen contents acting as reactant partners are not available in the course of the joining process, it is not possible to reach maximum build-up of the oxide layer during the process time. Within the framework of this paper, this is referred to as the non-saturation range. If on the contrary, the quantity of the available oxygen content was to be significantly more than the quantity necessary to reach maximum build-up of the oxide layer, the maximum oxide layer build-up would nevertheless still be dependent on the temperature. In this case, an increase in or a reduction of the oxygen contents would bear no effect on the oxide layer thickness in the joining process. Within the framework of this paper, this is referred to as the saturation range.

**Fig. 4** Oxide layer thicknesses upon oxygen content variations in a nitrogen atmosphere after the heat-up process

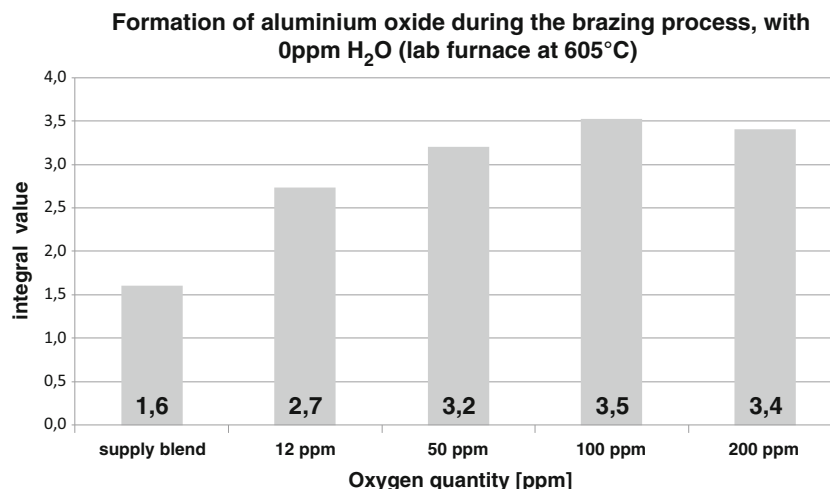
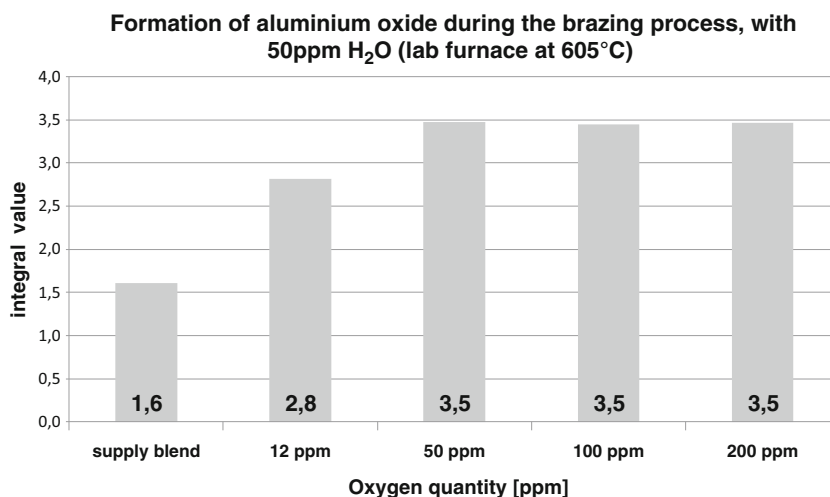


**Fig. 5** Oxide layer thicknesses subsequent to oxygen content variations in a nitrogen atmosphere with 50 ppm water, after the heat-up process



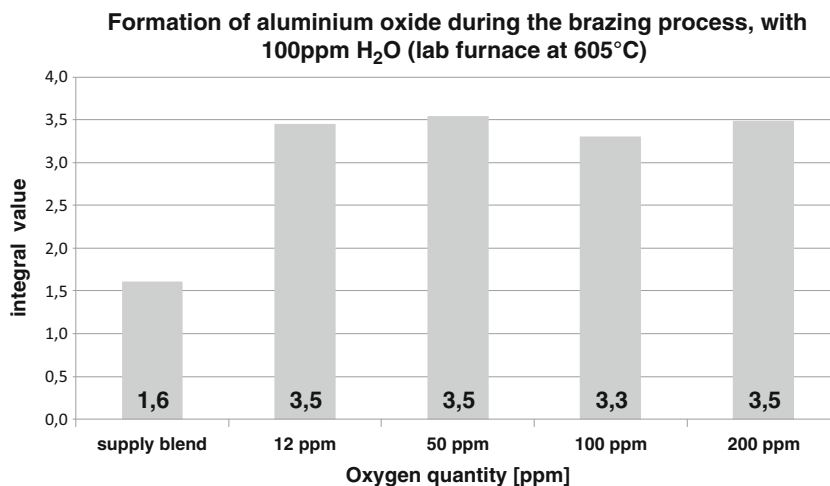
In order to be able to wield an effect on maximum oxide layer build-up by way of the oxygen and humidity contents, the relative substance concentration blends should not fall under the “saturation range” (to the right of the straight lines in Fig. 8). To this purpose, the straight lines drawn divide the “non-saturation range” from the “saturation range” (to the left of the straight lines). Within the saturation range, a reduction or an increase in the substance concentration blends will not influence the thickness of the oxide layer. To be able to have such an influence, it is necessary to shift into the non-saturation range. In this range, variations to the substance concentration blends will lead to variations in the thickness of the oxide layer. Therefore, any variations in the gas-shielded atmosphere produced for the joining process will wield an influence on the thickness of the oxide layer only in the event that the said variations occur within the non-saturation range. The saturation range as represented is to be held valid only for the recorded test data. The exact values need to be determined for each gas-shielded joining process, depending on the relative temperature, process time, and atmosphere.

**4 Influence of water vapor and oxygen in gas-shielded atmosphere and the resulting effects on brazeability**

Hereunder the brazing quality of test samples is evaluated, subsequent to glass furnace brazing, performed as previously in different atmospheres under otherwise similar conditions. Figures 9 and 10 illustrate the results of the respective brazing test runs. Upon comparing the joints between the V-shape and the base plate, differences in the brazed test sample fillet formation are clearly visible, which are reduced upon increasing the oxygen and humidity contents in the atmosphere.

Based on the test series performed on brazeability, it is demonstrated that humidity contents in the atmosphere yield a deteriorating effect on brazeability results. When compared directly with the oxygen atoms, the influence of humidity can be described as being stronger (see Fig. 10). In all of the test runs, the brazing of the test samples was practically fully completed in just about all of the atmospheric combinations, although there are some obvious differences in the fillet formation processes, whereby in all of the tests run under high humidity and oxygen concentration levels fillet formation

**Fig. 6** Oxide layer thicknesses upon oxygen content variations in a nitrogen atmosphere with 100 ppm water, after the heat-up process



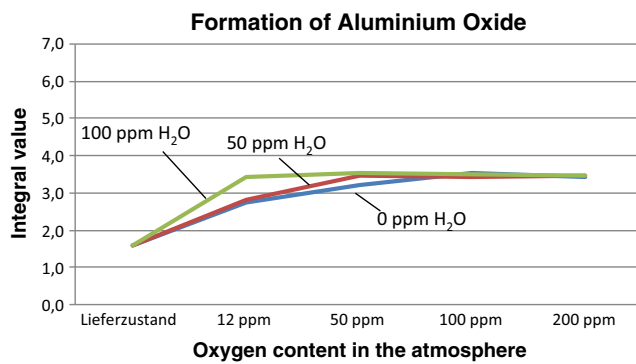


Fig. 7 Maximum build-up of the oxide layer thickness—Summary

remain rudimentary. In the presence of high humidity contents combined with high oxygen concentrations, the components are not moistened at all and there are also no apparent diffusion processes. No brazing joint is thus established in said components. Contrarily hereto, in virtually pure oxygen atmospheres, fillet formation is considerably conspicuous [2].

## 5 Influence of water on aluminium surfaces

In the experiments described above, the influence of atmospheric elements was examined. In the paper by Zähr [1], the primary cause is suspected to be the water evaporated by heating in the top layer of the aluminium surface. It is also not clarified whether humidity coming from the materials during the heating process occurs exclusively due to the dehydration of hydrated layers, or whether water is also

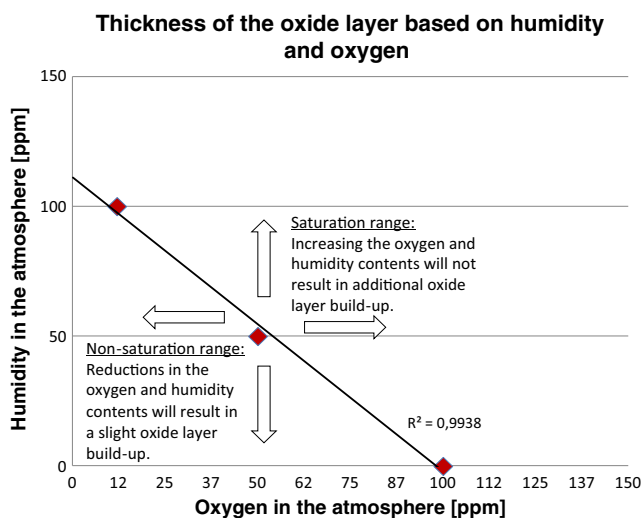


Fig. 8 Maximum oxide layer thickness, in relation to heating-up of the atmosphere

present in unbound form on the aluminium surface. With the help of the following experiment, knowledge should be obtained regarding the water absorption of aluminium surfaces. Here, the focus is on the following questions:

- Can water be embedded on the surface and to what depth is it embedded?
- What type of water bond is present on the surface after water treatment of up to 24 h at room temperature?

### 5.1 Determining the water absorption of aluminium surfaces

To be able to answer these questions, water treatment is performed with artificially modified water. This water is enriched with an oxygen isotope which can be detected using mass spectroscopy. In these so-called “tracer experiments”, isotopes are used which participate in reactions and can then be specifically analysed. The isotopes are thus used as marking elements. Due to the normally low quantity of isotopes, a reaction is not usually influenced. Tracers are often used in human diagnostics, but are also suitable for experiments in chemistry [14, 15]. Isotopes are elements with the same number of protons in the atomic nucleus, although they have a different number of neutrons. The isotopes of an element therefore have different mass numbers. The isotope  $^{18}\text{O}$  is one of the stable oxygen isotopes and is present naturally in water with a share of 0.2 %. As a result, there is no decay and it is also not radioactive, which considerably reduces the work required in testing.

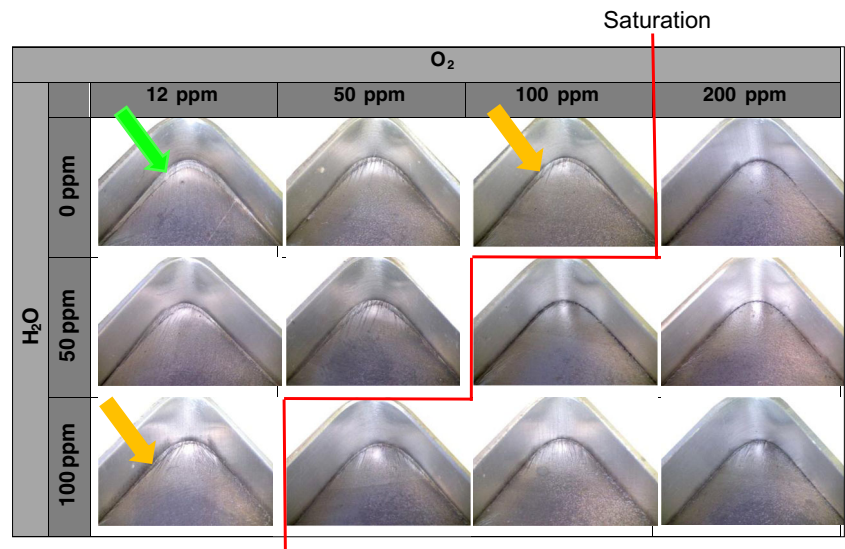
### 5.2 Test description

First of all, the samples undergo water treatment. For this purpose, the samples are sprinkled with  $^{18}\text{O}$  water (see Figs. 11 and 12) for a period of 5 min and 24 h. The share of the  $^{18}\text{O}$  atoms in the water used is increased from 0.2 to 97 %. The water treatment of the samples is done under a normal atmosphere and at room temperature. To prevent the fluid from evaporating, the samples are stored in closed containers.

#### 5.2.1 Evidence of water embedding

Direct evidence of water is not readily available. As a result, in the analysis, it is not the water molecules but the  $^{18}\text{O}$  atoms that are detected. Using the ratio of the detected  $^{18}\text{O}$  atoms to  $^{16}\text{O}$  atoms, it can be determined whether it is a natural ratio or an artificially altered ratio. The naturally occurring ratio is 1:0.002 (this corresponds to 0.2 % of  $^{18}\text{O}$  atoms). With  $^{18}\text{O}$  atoms which are additionally present from the water treatment

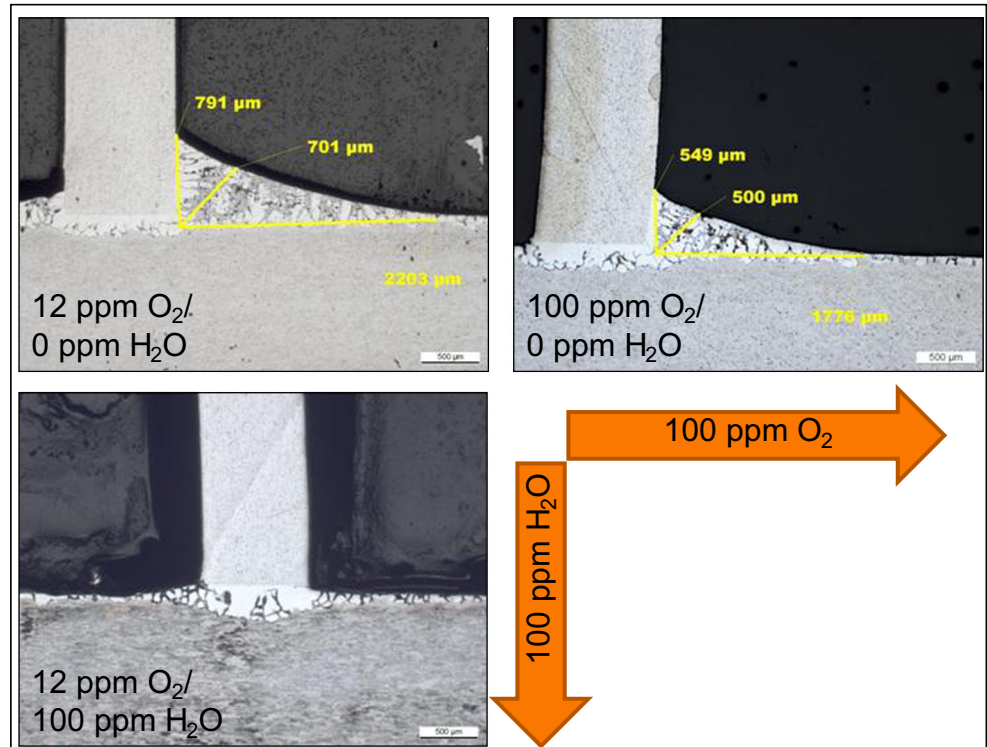
**Fig. 9** Brazing results on the angle test specimens—Overview



performed, the value is correspondingly higher. As an enrichment of the  $^{18}\text{O}$  atoms can only occur if  $^{18}\text{O}$  water is present on the surface or a reaction has occurred between the water and the elements, the evidence of  $^{18}\text{O}$  atoms can also be seen as evidence of the penetration of water. The depth to which the  $^{18}\text{O}$  atoms are detected in an unnatural ratio to the  $^{16}\text{O}$  atoms therefore corresponds to the depth of penetration of the water into the aluminium surface. It also applies that the higher the

number of  $^{18}\text{O}$  atoms in relation to  $^{16}\text{O}$  atoms, the more water is stored in the surface or the more water reacted with the surface, which can be used as an indirect indication of the amount of water which penetrated. The  $^{16}\text{O}$  atoms and  $^{18}\text{O}$  atoms are determined using the TOF-SIMS analysis. As this measuring procedure can only detect the upper molecule layers, a surface removal is performed by shooting the test point with Cs ions (sputtering). In this process, the surface

**Fig. 10** Sensitivity analysis of H<sub>2</sub>O and O<sub>2</sub> in the atmosphere [2]



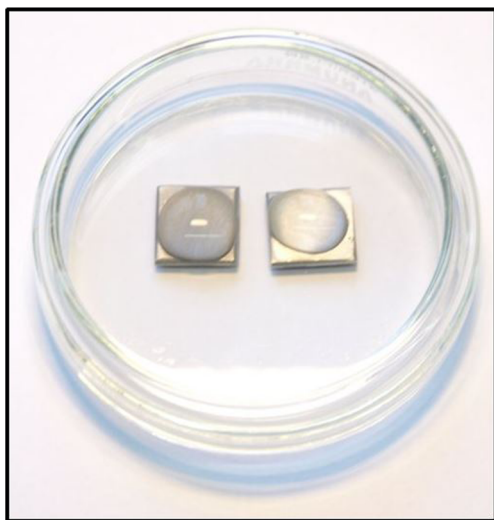


**Fig. 11** Samples sprinkled with  $^{18}\text{O}$  water [16]

removal is approximately 0.5–0.6 nm/s for pure aluminium, while for aluminium oxide the surface removal is several times lower. Due to the large difference in the surface removal, evaluation of the depth in the area of the surface is subjected to a potentially large error margin. Therefore, all depths are shown in connection with the sputter time.

### 5.2.2 Evidence of modified aluminium oxide

To obtain knowledge about the binding condition of the water in the aluminium surface, the ratio of aluminium oxide with embedded  $^{18}\text{O}$  atoms to aluminium oxide with embedded  $^{16}\text{O}$  atoms is determined. If there is neither a reaction with the aluminium nor the present aluminium oxide/hydroxide, then the natural ratio of 1:0.002 would exist, as would also be expected on untreated samples.



**Fig. 12** Ampullae with  $^{18}\text{O}$  water [16]

## 5.3 Test results

### 5.3.1 Detection of $^{18}\text{O}$ atoms on the surface of aluminium materials

The sample surface measurement with TOF-SIMS is done without surface removal. The initially analysed depth therefore corresponds to the upper 1–2 molecule layers. Table 2 shows the ratio calculated between the  $^{18}\text{O}$  atoms and the  $^{16}\text{O}$  atoms. Figures 13 to 16 graphically show the peak values of the respective measurements. The detected  $^{18}\text{O}$  atoms come from all molecules and molecule groups, which are located on the surface.

In the untreated sample, the detected  $^{18}\text{O}$  presence on the surface corresponds to the natural presence in water of 0.2 %. This shows that this method can be applied to measure the isotopes in the aluminium surface.

The sample which was water-treated for 5 min already shows a quantity of  $^{18}\text{O}$  atoms which is 210 times the natural level. In accordance with this, 42 % of the detected oxygen atoms in the surface already include the  $^{18}\text{O}$  isotope. The sample which was water-treated for 24 h showed an  $^{18}\text{O}$  atom share of 50 %. This means that even after water treatment of just 5 min there is clear water enrichment on the surface of the aluminium. A longer duration of the treatment only slightly increased the quantity of water in the surface. This allows us to presume that after just 5 min of immersion in water the outer layer is enriched with water and all pores and gaps are full, so that further water absorption in this area is only possible to a minor degree even after longer water treatment.

### 5.3.2 Modified aluminium oxide

Table 3 shows the ratio of aluminium oxide molecules to embedded  $^{18}\text{O}$  atoms compared to the ratio of aluminium molecules to embedded  $^{16}\text{O}$  atoms. This, therefore, shows the share of modified aluminium oxide molecules for different types of water treatment.

### 5.3.3 Depth analysis of the aluminium surface after 5 min immersion in water

Figure 13 shows the progress of the signal lines of a sample, which was treated for 5 min with water containing  $^{18}\text{O}$ . The evaluation is done according to the following signal lines.

- Natural aluminium oxide
- $^{18}\text{O}$  modified aluminium oxide
- $^{16}\text{O}$  atoms
- $^{18}\text{O}$  atoms

In the diagram, please note that the signal lines for “ $^{16}\text{O}$ ” and “ $^{18}\text{O}$ ” comprise all  $^{16}\text{O}$  atoms and  $^{18}\text{O}$  atoms which are



**Table 2** Share of the O18 atoms in the surface [16]

	No water treatment	5 min of water treatment	24 h of water treatment
Ratio ( $^{18}\text{O}/^{16}\text{O}$ )	0.002	0.42	0.50

embedded in the molecules. This means that the difference between the present intensities of  $^{18}\text{O}$  and  $\text{Al}^{18}\text{O}$  cannot be definitively clarified. The difference could, on the one hand, be due to hydrated oxides, but, on the other hand, also due to trapped water in the surface, which was not released during the evacuation in the measuring equipment. The latter should, however, play a subordinate role.

Figure 13 shows a strong initial drop in  $^{18}\text{O}$  and  $\text{Al}^{18}\text{O}$  signals, followed by an even, slow drop in intensity. The intensity of the  $^{18}\text{O}$  signal line is one scale higher than the  $\text{Al}^{18}\text{O}$  signal line. Figure 14 shows the signal lines from Fig. 13 in a different display and a higher resolution. Here, the maximum intensity values of the displayed signal lines have been scaled to one. As a result, the high increase in  $^{18}\text{O}$  atoms in the first period of sputter time (here represented for 3 s) is visible, followed by a steep initial drop, which changes into a flat and even drop in signal intensity after approximately 20 s. The signal line of the modified aluminium oxide is very similar, although with an offset of approximately 2 s of sputter time.

The signal lines of the natural aluminium oxide, on the other hand, rise in the first few seconds slightly more

gradually to the maximum value, which occurs at a later period of sputter time (here represented by approximately 8 s). This shows that the outermost layer was modified during water treatment from  $\text{Al-O}$  to  $\text{Al}^{18}\text{O}$ . Over the course of the analysis, the intensity of this  $\text{Al-O}$  signal line falls constantly with a minor decrease in intensity.

#### 5.3.4 Depth analysis of the aluminium surface after 24 h immersion in water

Figure 15 visualizes the progression of the signal lines of a sample, which was treated for 24 h with water containing  $^{18}\text{O}$ . This shows, as the 5-min sample has already shown, a strong initial drop in  $^{18}\text{O}$  and  $\text{Al}^{18}\text{O}$  signals. However, this is less pronounced than in the 5-min sample. In the 24 h probe, both signal lines show a generally higher intensity, which indicates that the water penetrated to a greater depth.

Figure 16 depicts the signal lines of the 24 h sample again scaled to one. The rise of the  $^{18}\text{O}$  signal line, like in the 5-min sample, reaches the maximum level within a first period of sputter time (here represented by 3 s of sputter time), which, contrary to the 5-min sample, does

**Fig. 13** (Left) TOF SIMS analysis—5 min water treatment [16]—first period of sputter time

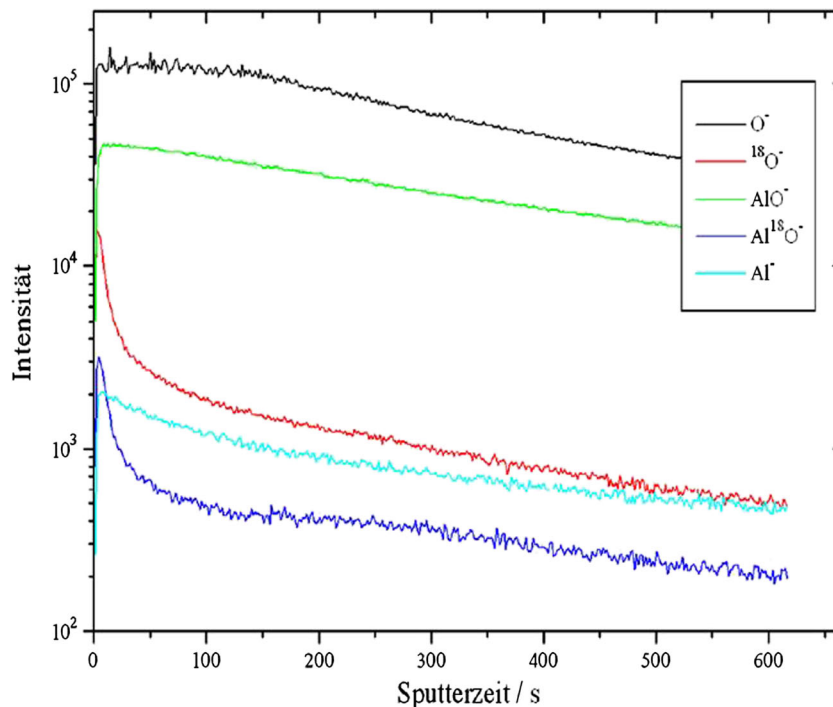


**Table 3** Share of the  $^{18}\text{O}$  atoms in aluminium oxide [16]

	No water treatment	5 min of water treatment	24 h of water treatment
Ratio ( $\text{Al}^{18}\text{O}/\text{Al}^{16}\text{O}$ )	0.0015	0.49	0.60

not drop steeply but remains at this level for approximately 3 s and then falls much slower to an intensity level of approximately 0.6. From this intensity, the signal line drops by a comparable amount to the 5-min sample. The rise of the Al-O signal line is again flatter compared to the 5-min sample, which is due to a larger number of  $^{18}\text{O}$  modified molecules. This is also shown by the wider peak of the  $\text{Al}^{18}\text{O}$  line.

## 6 Water retention model

From the water immersion tests, already published, it is known that during water treatment in a period of up to 24 h at room temperature, there is no growth in the aluminium oxide layer and only very low growth in the hydrated layer [17]. The hydrated top layer is less than 2 nm thick, both before and after the water immersion [17]. From these water immersion tests, it is known that after the water immersion

and the subsequent thermal treatment the brazability drops the longer the water treatment lasts.

Already published, oxide layer thickness tests on water-treated samples show a clear difference compared to untreated samples after thermal treatment and a water treatment for 5 min. The difference in the thickness of the oxide layer after 5 min water immersion and 24 h water immersion with subsequent thermal treatment is only small [17].

This shows that the water immersion occurs in the outer layer of the aluminium surface. The difference between the embedded quantities of water after 5 min of water treatment, compared to 24 h of water treatment, is very low. After 24 h of water treatment, the water penetrates a much greater depth into the surface than in the 5 min water treatment (see Fig. 17).

As the embedded quantity of water in the outer layer is virtually independent of the duration of the water immersion, it can be concluded that the available cavities in the outer layer are filled with water and therefore this layer is saturated with water. A further increase in the water immersion during longer water treatment occurs by water penetrating the lower layers. Here, however, the water quantities are less than in the direct surface.

After a short water treatment, the outer layer is already saturated, which leads to a clear influence on the oxide layer during thermal treatment. An increase in the duration of the water treatment only causes a minor increase in the water quantity and therefore only a minor further increase in the

**Fig. 14** (Right) TOF SIMS analysis—5 min water treatment (standardized scale) [16]—first period of sputter time

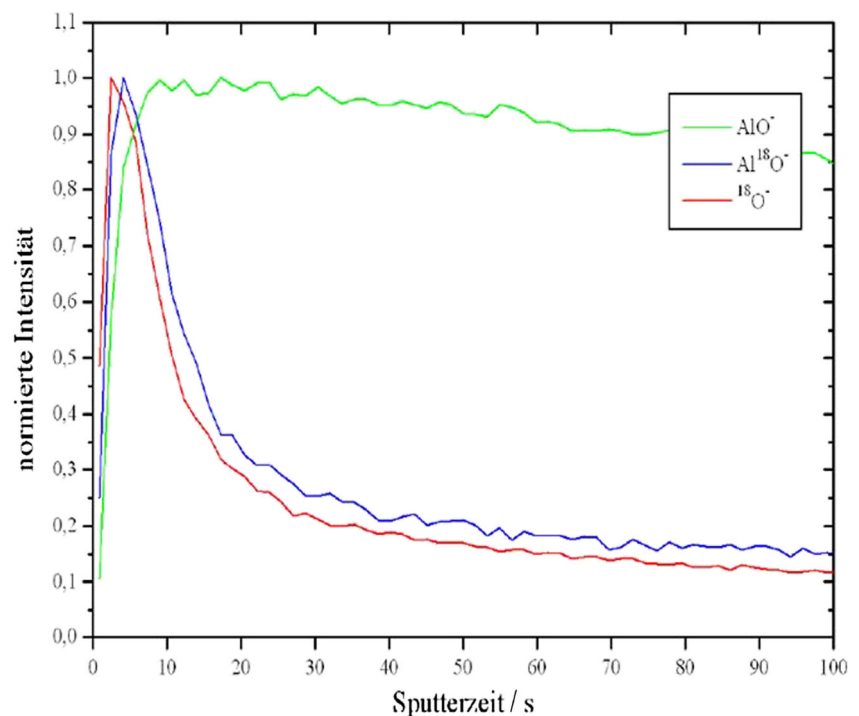


**Fig. 15** (Left) TOF SIMS analysis—24 h water treatment [16]—first period of sputter time

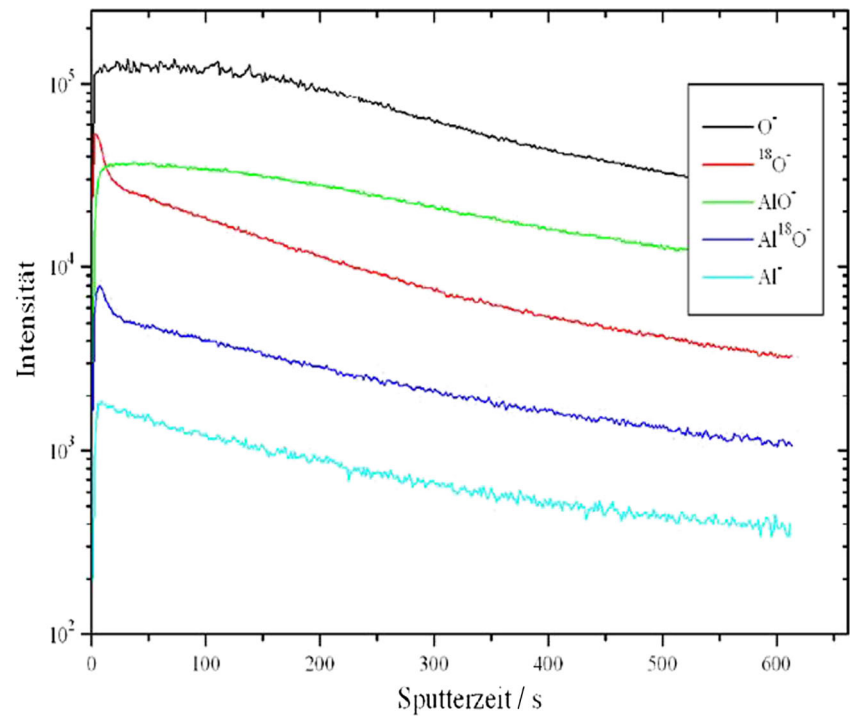


**Fig. 16** (Right):TOF SIMS analysis—24 h water treatment (standardized scale) [16]—first period of sputter time

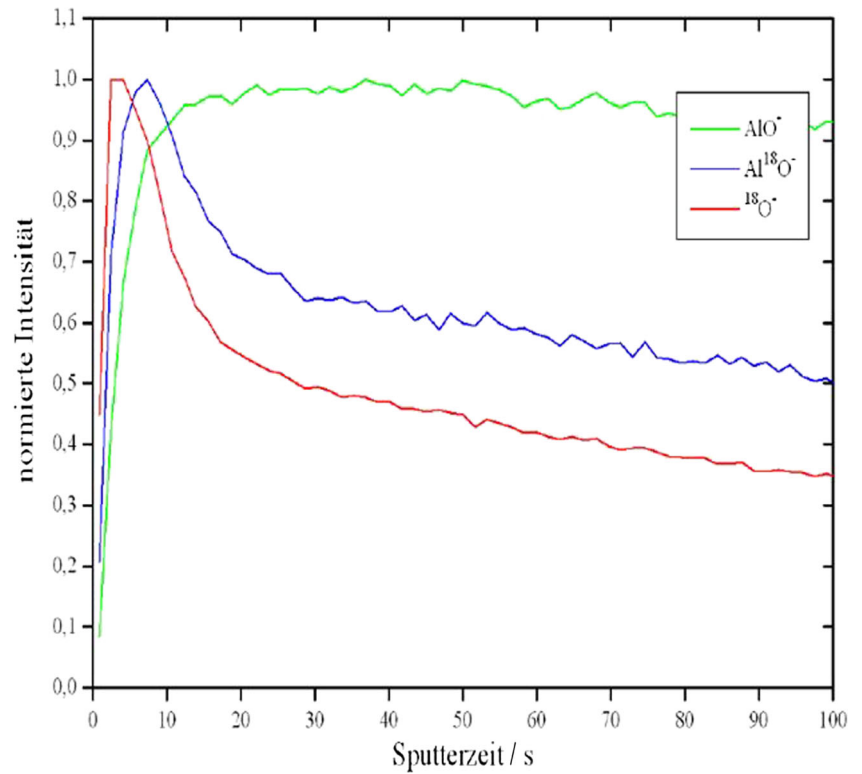
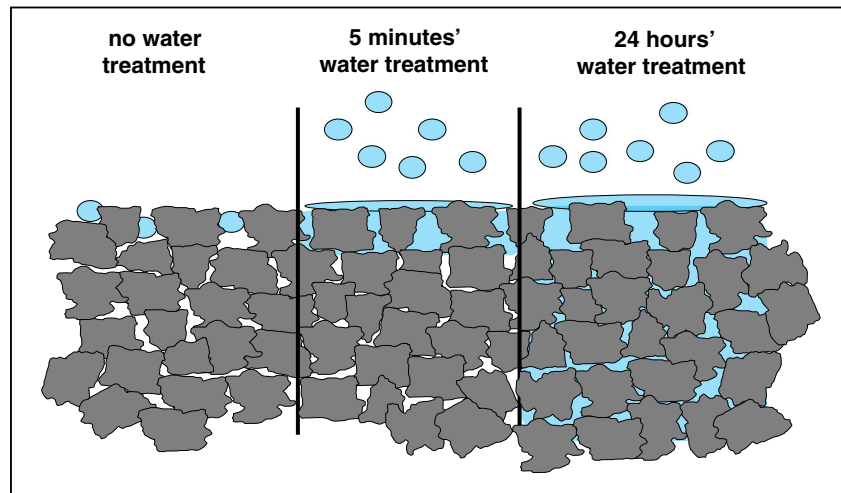


**Fig. 17** Water retention in the aluminium surface



influence on the oxide layer during thermal treatment. It is, therefore, possible to reach the following conclusions:

1. Water can be embedded in the aluminium surface due to water treatment.
2. The water embedded in the surface is mainly not bound due to a reaction to hydroxide.
3. The duration of the water treatment is of minor importance for the quantity of embedded water.
4. The quantity of water embedded during 5 min already has a clear influence on the thickness of the oxide layer during the heating process.

## 7 Discussion of results

### 7.1 Test results

The test results show a clear influence of moisture on the oxidation process. Here, it can be stated that moisture has no influence on the maximum possible oxide layer thickness. This is purely dependent on the temperature. Furthermore, it can also be stated that moisture in the atmosphere can considerably reduce the amount of oxygen, which is necessary to achieve the maximum oxide layer thickness (under otherwise identical conditions), under the condition that the processes run in the aforementioned “unsaturated area”.

The test results with respect to brazeability show a clear drop in brazeability as the share of moisture in the atmosphere increases. Here, the influence of moisture in the atmosphere is stronger than the influence of oxygen. This confirms Zähr’s conjecture [1] that moisture in the atmosphere plays a primary role in the brazeability of aluminium materials.

Furthermore, it can also be shown that a clear general improvement in brazeability can again be achieved due to the large brazed fillets under high-purity inert gas

atmospheres, with regards to moisture and oxygen. In inert gas atmospheres without moisture and low oxygen values (12 ppm), the brazed samples showed much stronger brazed fillets, compared to the working range of the current inert gas brazed processes.

### 7.2 Conclusions from the water retention model

Due to the immersion of water in the aluminium surface, it can be concluded that this water escapes during the heating process and causes the local moisture in the brazed atmosphere to increase. According to the test results on the moisture in the atmosphere, this has a clear influence on brazeability. It can, therefore, be determined that ingress of water into the inert gas atmosphere can mainly occur in three ways:

1. The occurrence of moisture as a reaction product in accordance with the known dehydration function during the conversion of hydroxide into crystalline aluminium oxide during thermal treatment.
2. By evaporating unbound embedded water, which has become embedded in the surface even after short water treatment.
3. Due to moisture already present in the inert gas.

## 8 Outlook

In this thesis, the influence of moisture on brazeability has been extensively examined. It shows that moisture in the brazed atmosphere represents a primary factor regarding brazeability, which has to date not been considered. This knowledge opens up other fields of research for science to support and further develop the industrial use of brazing

technology on aluminium materials. An open question for further investigation is what may be the role of the characteristics of aluminium oxide film during water treatment, including microstructure and chemical compositions, compared to the importance of water retention, initiating the oxide growth during later brazing process as described in this paper.

## References

- Zähr J (2010) Einfluss des Oberflächenzustandes auf das thermische Fügen. PHD-Thesis, Dresden: TU Dresden
- Lohrey M, Fuessel U, Tuerpe M (2013) Behaviour of the aluminium oxide layer during heat treatment and the resulting effect on brazeability. DVS Media, Berichte Band 293, Aachen
- Wefer K, Misra C (1987) Oxides and Hydroxides of Aluminium. n.b. : Alcoa Laboratories
- Wittke K, Fuessel U (1996) Kombinierte Fügeverbindungen. Springer Verlag, Heidelberg, ISBN 3-540-54469-0
- Altenpohl D (1965) Aluminium und aluminiumlegierungen. Springer Verlag, Zürich
- Kammer C (1998) Aluminium-Taschenbuch. Aluminium-Verlag, Düsseldorf, ISBN 3-87017-241-X
- Winston R, Uhlig's R (2000) Corrosion Handbook. Wiley-Interscience, Inc, New Jersey, ISBN 0-471-78494-x
- Ostermann F (2007) Anwendungstechnologie Aluminium. Springer Verlag, London, ISBN 3540238824
- Altenpohl D (1955) Korrosionsschutz des Aluminiums durch natürliche oder verstärkte Oxidschichten: Neuere Untersuchungen
- Jelinek T (1997) Oberflächenbehandlung von Aluminium. Eugen Leuze Verlag, Saulgau
- Vargel C (2004) Corrosion of Aluminium. Elsevier Ltd, Oxford, ISBN 0-080-33395-4
- Wehner I (1999) Oxidation von Quasikristallen und kristallinen Phasen im System Al-Cu-Fe. Düsseldorf : VDI
- Hauffe K (1956) Oxidation von Metallen und Metalllegierungen. Springer Verlag, Frankfurt
- Prescott R, Graham MJ (1991) The formation of aluminium oxide scales on high-temperature alloys. Institute of microstructural sciences national research council of canada, Canada
- Heumann T (1992) Diffusion in metallen. Springer Verlag, Berlin, ISBN 3-540-55379-7
- Analytik OFG (2012) Analysen an mit 180-Wasser behandelten Al-Blechen (unveröffentlichter Bericht). Münster : s.n
- Lohrey M, Fuessel U, Tuerpe M (2012) Protective atmosphere brazing of aluminium material. Fraunhofer IWS, Symposium: Tailored Joining, Dresden